

Preliminary design of a heavy ion beam probe diagnostic for the National Spherical Torus Experiment

F. H. Mull, T. P. Crowley, P. M. Schoch, and K. A. Connor
Rensselaer Polytechnic Institute, Troy, New York 12180

(Presented on 10 June 1998)

The preliminary design of a heavy ion beam probe (HIBP) for the National Spherical Torus Experiment (NSTX) is presented. The primary purpose of the diagnostic would be to measure density and electric potential fluctuations and steady state potential profiles. A secondary purpose is magnetic equilibrium and fluctuation measurements. HIBP particle trajectories have been calculated for a double null discharge case. The key HIBP measurements can be made with the injection point—detection point combination which is presented, including a radial scan line at a single energy (for potential profile measurements), poloidally aligned sample volumes (for poloidal wavenumber measurements), and coverage of a large fraction of the upper low field quadrant of the plasma. In addition, the injection point can be combined with new detectors for radial array measurements (for density fluctuation and/or magnetic measurements). Due to a large range of angles at the detector, up to 23° poloidal angle range and a 6° toroidal angle range, a secondary sweep system will be necessary for NSTX. © 1999 American Institute of Physics. [S0034-6748(99)74101-8]

I. PRINCIPLE OF HEAVY ION BEAM PROBING

A heavy ion beam probe (HIBP) diagnostic will provide a number of unique measurements of importance to National Spherical Torus experiment (NSTX) science. An HIBP can measure electric potential (equilibrium and fluctuations), density fluctuations, and magnetic field (equilibrium and fluctuations). In addition, the potential and density fluctuation measurements can be used to obtain the particle flux caused by electrostatic fluctuations. The potential and density measurements have been demonstrated on many devices,¹ and this design focuses on these measurements. The magnetic field measurements have been demonstrated on TEXT^{2,3} and may be practical on NSTX, although this requires further study. This article describes the preliminary design work on the NSTX HIBP.

The basic principle of heavy ion beam probing is to inject a beam of singly charged ions, called primaries, into the plasma, as shown in Fig. 1. As the ions pass through the plasma, they are further ionized (usually by electrons) to produce doubly charged ions, called secondaries.

In the usual mode of HIBP operation, a small aperture energy analyzer placed outside the magnetic field accepts a narrow secondary beam. These secondaries originate in a small region of the probing beam known as the sample volume. The sample volume position can be changed along a curved line by redirecting the probing beam with electrostatic sweep plates. This process typically takes 10 ms for a complete scan. Different lines are selected by changing the ion energy (accelerator voltage). The amount of secondary ion current collected by the analyzer is proportional to the electron density in the sample volume, the beam energy depends on the electric potential in the sample volume, Φ_{sv} , and the out of plane motion of the beam depends on the

magnetic vector potential A_ϕ . These quantities are independently measured by our detectors.

The electric potential measurement is based on conservation of energy. As the primary beam passes through the plasma, the total energy is conserved. When a primary ionizes, an electron is stripped off, removing a potential energy of $-e\Phi_{sv}$ (and negligible kinetic energy) where $-e$ is the electron charge. The secondary beam energy is therefore $e\Phi_{sv}$ higher than the primary beam. The secondary beam energy is measured using a parallel plate energy analyzer in

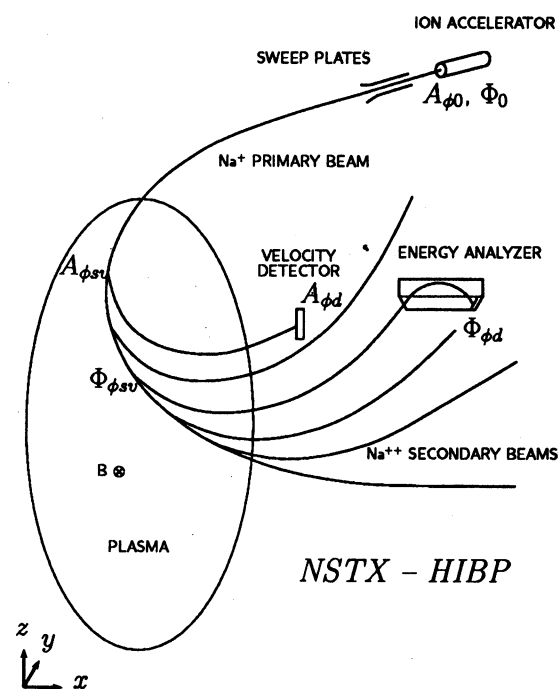


FIG. 1. Principle of heavy ion beam probing.

i_{LU}	i_{RU}
i_{LD}	i_{RD}

$$i_U = i_{LU} + i_{RU}$$

$$i_D = i_{LD} + i_{RD}$$

FIG. 2. Close-up view of the energy analyzer split-plate detector.

which the beam deflection depends on its energy. This deflection and hence the beam energy is determined from the ratio i_U/i_D where i_U and i_D are the upper and lower split plate currents, as in Fig. 2.

The beam deflection in the toroidal plane can be measured from the ratio i_L/i_R in Fig. 2 and this is a measure of the toroidal component of the magnetic vector potential, A_ϕ , or the poloidal magnetic field B_{pol} . A better detection method is based on a velocity detector as will be discussed later.

II. NSTX DESIGN

Compared to previous HIBP experiments, NSTX has a significantly larger plasma size, and therefore, larger attenuation for beams of identical energy and mass. The relative port size to plasma size is also smaller than in most previous experiments. It also has a much lower magnetic field (0.3 T on the geometric axis) than recent experiments and the ratio of poloidal to toroidal magnetic fields is much larger than in a typical tokamak. Similar issues are present in the HIBP experiment for the Madison Symmetric Torus (MST) reversed field pinch that is under construction.⁴ In general, the design issues are not as difficult on NSTX.

The beam energy required to get good trajectories for an HIBP experiment scales roughly as $a^2 B^2 / M$ where a is the device size, B is the magnetic field strength, and M is the probing ion mass. Although a is much larger in NSTX than in previous experiments such as TEXT, B is smaller by a larger ratio. Thus, we can use the TEXT accelerator with lower mass ions on NSTX. The lower mass ions have smaller ionization cross sections which compensates for the longer path lengths resulting in a reasonable beam attenuation and signal strengths. The large ratio of poloidal to toroidal magnetic field results in significant toroidal beam deflections. Injection conditions which partially compensate for this have been chosen. Secondary sweep plates to compensate for some of the motion will also probably be necessary.

System design is also constrained by the desire to use existing equipment as much as possible. The 500 kV accelerator from the TEXT HIBP experiment has been identified as the best choice for accelerator. Either the ATF or TEXT-U energy analyzers can be used along with bending systems from TEXT and TEXT-U.

The preliminary design has been done with a trajectory code that solves the Lorentz force equation neglecting the electric field.

In this study the equilibrium magnetic field assumed is that for a double null discharge (Case 0128B). A single ion

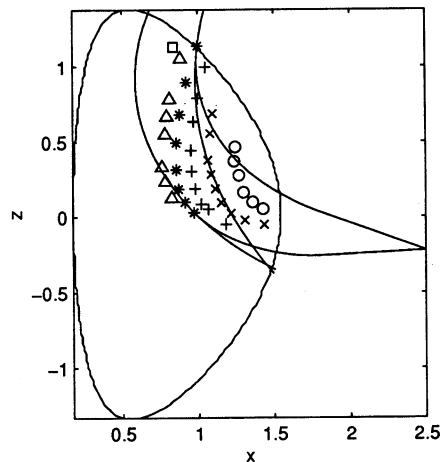


FIG. 3. Scan lines at varying energies illustrating plasma coverage.

accelerator position and energy analyzer position pair has been determined that allows reasonable plasma coverage. Using a 510 keV sodium beam, a scan can be achieved that extends from the plasma edge almost to the magnetic axis, as shown in Fig. 3. The starred points represent this scan line. The primary and secondary beams corresponding to the edge and axis sample volumes are also shown. The additional points represent scan lines at other energies. The lowest energy scan, denoted by circles, resulted from a 255 keV sodium beam. The highest energy point, represented by a square, corresponds to a 685 keV sodium beam. Using the energy mass scaling above, this is equivalent to a 400 keV potassium beam. The 500 kV (nominal) TEXT accelerator can reach all points up to the 510 keV scan line shown in Fig. 3 using sodium ions, since the maximum accelerator voltage is 545 kV. Higher energy points will require potassium beams.

Figure 4 shows the view from above of the 510 keV scan line illustrating the toroidal deflection of the beam. As expected, the motion is significantly more than in a conventional tokamak experiment, but not excessively so. The motion also forces the detector position used in the calculations to be displaced toroidally from the port. The HIBP experi-

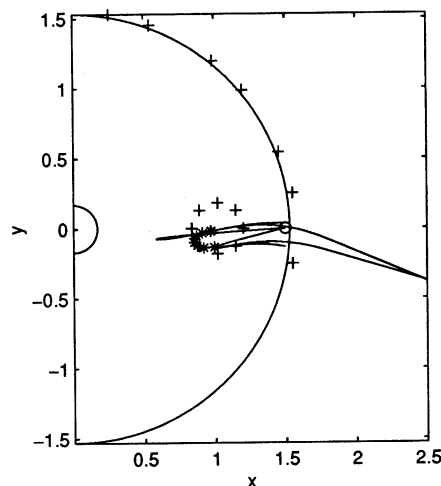


FIG. 4. View of scan line from above.

ment will therefore be limited to a single current direction since reversing the current moves the beam in the opposite direction. An advantage of the displacement is that the HIBP analyzer will be less of an obstruction to other diagnostics located on the same port.

The sample volumes in Fig. 3 have injection angles of $\theta = 22^\circ$ to 38° and $\phi = -4^\circ$ to -14.5° where θ is the angle with respect to the z axis and ϕ is the toroidal angle. These angle ranges can be achieved with conventional electrostatic sweep plates. The 500 keV accelerator has to be mounted either horizontally or vertically. With a horizontal mounting, a dc beam deflection of 60° is needed and this can be obtained by a dc sweep of 8° combined with an existing 68° deflector from TEXT-U.

The angle ranges at the detector for the scan line are 23° poloidally and 6° toroidally. This range is larger than desired for good operation and hence secondary sweep plates will probably be necessary. The reason for the large required angle range is probably due to the need to keep the injection and detection points close to the plasma since the size of the ports, relative to plasma size, is small. Secondary beamline sweep plates are not yet a standard HIBP characteristic, although they have been successfully used on the Compact Helical System (CHS)⁵ and are part of the MST HIBP design.⁶

III. BEAM ATTENUATION AND SIGNAL LEVELS

The effective ionization cross section for the 510 keV sodium ions used in the scan line peaks at a value of $\sigma = 1.3 \times 10^{-20}$ when $T_e = 800$ eV. For a plasma density of $n_e = 3 \times 10^{19} \text{ m}^{-3}$, this results in a mean free path of $\lambda_{\text{mfp}} = 2.6$ m, indicating good beam penetration.

The measured current at the detector is given by

$$I_s = \kappa \frac{q_s}{q_p} I_0 F_p F_s \sigma_{\text{ion}} l_{\text{sv}} n_e(r_{\text{sv}}),$$

where I_0 is the initial primary current injected into the plasma, σ_{ion} is the ionization cross section for primary to secondary ions, l_{sv} is the sample volume length, q_p and q_s are the primary and secondary charge states, $n_e(r_{\text{sv}})$ is the electron density at the sample volume, κ is a multiplying factor between 1 and 10 due to electron emission from the detector plates, and F_p and F_s represent primary and secondary beam attenuation and are given by

$$F_j = \exp(-\sigma_j n_e dl_j),$$

where $j = p, s$ for primary and secondary attenuation, σ_j represents all ionization processes from a given charge state, and the integrals are evaluated along the trajectory.¹

A rough estimate of the signal level for the sample volume near the magnetic axis in the scan line shown in Fig. 3 is obtained by assuming a constant plasma density ($n_0 = 3 \times 10^{19} \text{ m}^{-3}$) and temperature ($T_e = 1$ keV). We also assume $I_0 = 100 \mu\text{A}$, $\kappa = 5$, $l_{\text{sv}} = 5$ mm, $l_p = 1.5$ m, $l_s = 0.6$ m, and $\sigma_2 = \sigma_1/3$. The expected signal level is 1000 nA which is much larger than the broadband noise level of 1–2 nA.

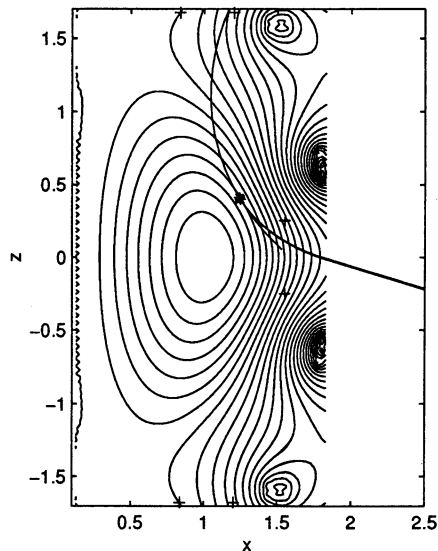


FIG. 5. Poloidal alignment of sample locations.

IV. POTENTIAL, DENSITY, AND PARTICLE FLUX MEASUREMENTS

Potential measurement accuracy of 100 V between two sample volumes has been demonstrated in previous experiments and is expected for NSTX. Accuracy in electric field measurements will then depend on the scale length of the potential structure.

Potential fluctuation measurements at a single sample volume can be obtained with much higher accuracy than the profile measurements. The measurement is limited by the broadband electronic noise and counting statistics. These yield a noise level of 1–2 nA for 0–500 kHz. For the scan line point nearest the axis and the energy analyzer used on Advanced Toroidal Facility (ATF), a $\bar{\phi}$ root mean square (rms) of 3.5 V will have a signal to noise ratio of 1. Since the noise spectrum is flat, the sensitivity to a 100 kHz wide fluctuation is approximately 0.7 V rms.

In order to determine particle flux, the poloidal wavenumber of the potential fluctuations is also needed. This is obtained by measuring phase shifts between two sample volumes displaced poloidally from one another. Multiple sample volumes are obtained using multiple entrance slits and they are poloidally aligned when the primary beam is tangent to the flux surface. Figure 5 shows an example, using a 255 keV sodium beam, of this alignment. We do not know yet over what range of radii we can obtain this alignment.

Density fluctuation sensitivity is simply the ratio of the noise level to the total signal. For the center point of the scan line, we expect a sensitivity of \bar{n}/n of 0.15% for 500 kHz bandwidth fluctuations and 0.03% for 100 kHz fluctuations.

Initial sample volume size calculations assuming an effective beam radius of 2 mm (a very well focussed beam) indicate that sample volume dimensions range from 1.5 cm in the plasma center to 5 cm at the plasma edge. These sample volumes will be sensitive to fluctuations with $k < 2 \text{ cm}^{-1}$ and 0.6 cm^{-1} , respectively. It should be noted that these result are still tentative at this point.

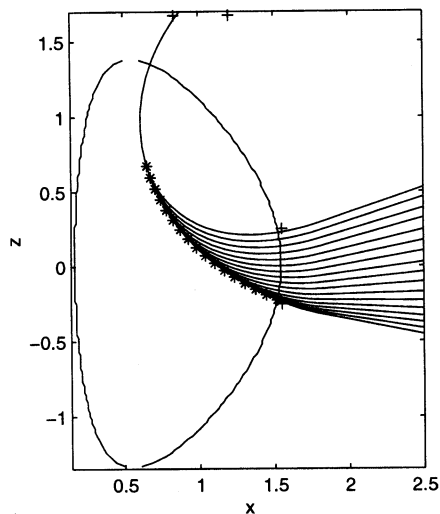


FIG. 6. Radial profile using an array velocity detector.

V. MAGNETIC VECTOR POTENTIAL AND FIELD MEASUREMENT

In an axisymmetric system, conservation of angular momentum,

$$p_{\phi} = MRv_{\phi} + qRA_{\phi}$$

can be used to determine $A_{\phi sv}$ by measuring v_{ϕ} where ϕ indicates the toroidal coordinate, R is the major radius, A is the vector potential, and v is the beam velocity. This is similar to how Φ_{sv} is determined by measuring the beam energy. In order to make this measurement work, a velocity detector should be placed inside the toroidal field coils so that the beam is detected before passing through the large nonsymmetric ripple field at the coils. A velocity detector is not a standard HIBP technique, however, such a detector was used on a hollow cathode arc experiment and successfully saw changes in beam velocity due to magnetic field changes.⁷ This detector was not located in the magnetic field, nor was it exposed to the levels of ultraviolet (UV) radiation expected on NSTX. Therefore, development work would be required to implement this feature. The approach in the design study is to allow the possibility for addition of velocity detectors at a later date. In particular, an array of detectors that could monitor all radial positions simultaneously is desirable. Fig-

ure 6 shows a set of 425 keV sodium beam trajectories for which this could be obtained with the existing input location.

A lesser alternative for magnetic measurements is to measure the toroidal beam displacement in the standard HIBP analyzer as previously mentioned. This measurement is sensitive to the field along the beam trajectory as well as at the sample volume. Nevertheless experiments and extensive computer simulations on TEXT have shown that the local signal is a large fraction of the total signal, and this allows one to obtain the equilibrium and fluctuating field as a function of radius.

VI. DISCUSSION

Using existing ports a fairly standard heavy ion beam probe diagnostic system can be installed on NSTX using an existing 500 kV ion accelerator. A scan extending from the plasma edge almost to the magnetic axis can be obtained with a single energy ion beam. By varying the ion energy, the upper low field quadrant of the plasma can be covered. Because of the large range of angles at the detector, a secondary sweep system will be necessary. The detection point is to the side of the port, as seen in Fig. 4, allowing room for other diagnostics to share the same port.

ACKNOWLEDGMENTS

Research supported by the U.S. Department of Energy. The magnetic fields were supplied to us by D. Strickler of ORNL. We would like to acknowledge helpful discussions with R. Kaita, D. Johnson, and S. Kaye of PPPL.

¹T. P. Crowley and the Rensselaer Plasma Dynamics Team, IEEE Trans. Plasma Sci. **22**, 291 (1994).

²V. J. Simcic, T. P. Crowley, P. M. Schoch, A. Y. Aydemir, X. Z. Yang, K. A. Connor, R. L. Hickok, A. J. Wootton, and S. C. McCool, Phys. Fluids B **5**, 1576 (1993).

³J. G. Schwelberger, T. P. Crowley, K. A. Connor, and P. M. Schoch, Rev. Sci. Instrum. (accepted for publication).

⁴U. Shah, K. A. Connor, J. Lei, P. M. Schoch, T. P. Crowley, J. G. Schatz, and Y. Dong, Rev. Sci. Instrum. (these proceedings).

⁵A. Fujisawa, H. Iguchi, S. Lee, T. P. Crowley, Y. Hamada, S. Hidekuma, and M. Kojima, Rev. Sci. Instrum. **67**, 3099 (1996).

⁶J. Lei, T. P. Crowley, U. Shah, P. M. Schoch, K. A. Connor, and J. G. Schatz, Rev. Sci. Instrum. (these proceedings).

⁷G. Tonetti, 11th European Conf. on Controlled Fusion and Plasma Physics, 1983 (unpublished).